
Mapping recharge from space: roadmap to meeting the grand challenge

Dara Entekhabi · Mahta Moghaddam

Abstract Fields of diffuse recharge flux play pivotal roles in: (1) linking surface and subsurface hydrologic systems, (2) controlling the biogeochemistry of terrestrial systems, and (3) determining the sustainability of well withdrawals from aquifers. This hydrologic flux is intimately related to the distribution and functioning of vegetation cover and type. In turn, it also plays a significant role in the distribution of vegetation. Until now, recharge has been mostly estimated as residual of either surface or subsurface water balance. In situ instruments for measurement of this quantity are difficult to implement and maintain. Long-term and spatially explicit (mapped) monitoring of recharge flux have been elusive goals. A review is presented of the possible spaceborne and airborne remote sensing and data interpretation techniques that may address the grand challenge of recharge mapping on large scales. The approaches rely on microwave remote sensing in order to measure land surface states in the presence of atmosphere and vegetation cover that attenuate and disturb the signal as it travels from the surface to the sensor. The emphasis is on radar systems that also have beneficial ground spatial resolution characteristics. Finally, examples of two candidate space-borne systems are presented as feasible approaches to the required measurements.

Résumé Les aires de recharge diffuse jouent des rôles pivots dans : (1) la jointure entre les systèmes de surface et de sub-surface, (2) le contrôle de la biogéochimie des

systèmes terrestres, et (3) la détermination de la durabilité des débits des puits soustraits aux aquifères. Ce flux hydrologique est intimement lié à la distribution et au fonctionnement des couvertures végétales et des types de végétaux. Inversement, la recharge joue un rôle significatif dans la distribution de cette végétation. Jusqu'à présent, la recharge a été essentiellement estimée en tant que résidu des bilans hydrologiques de la surface ou de la sub-surface. Les instruments in-situ mesurant cette quantité sont difficiles à installer et à maintenir. Les surveillances sur le long terme et spatialement explicites (cartographiées) des flux de recharge ont été des objectifs difficiles à atteindre. Une revue est présentée des possibles techniques de télédétection et des techniques d'interprétation permettant d'approcher le grand défi de la cartographie de la recharge à grande échelle. Ces approches reposent sur la télédétection à micro-ondes pour mesurer les états de la surface du sol en présence d'une atmosphère et d'une couverture végétale qui atténuent et perturbent le signal lorsque ce dernier voyage de la surface au capteur. L'accent est mis sur les systèmes de radar qui ont également des caractéristiques bénéfiques de résolution spatiale du sol. Finalement, les exemples de deux candidats aux systèmes spatiaux sont présentés comme de possibles approches aux mesures requises.

Resumen Las áreas de flujo de recarga difusa tienen papeles esenciales en: (1) Poner en contacto sistemas hidrológicos superficiales y subterráneos, (2) controlar la biogeoquímica de sistemas terrestres, y (3) determinar la sostenibilidad de la extracción de los acuíferos mediante pozos. Este flujo hidrológico está íntimamente relacionado a la distribución y al funcionamiento del tipo y cubierta de vegetación. A su vez, también juega un papel significativo en la distribución de la vegetación. Hasta ahora la recarga ha sido principalmente estimada como el residuo, tanto del balance de agua superficial, como del subterráneo. Los instrumentos in situ para la medida de esta cantidad, son difíciles de instalar adecuadamente y de mantener. El monitoreo espacialmente explícito (cartografía) y de largo plazo, del flujo de la recarga, ha sido una meta difícil de alcanzar. Se presenta una evaluación de las técnicas de interpretación de datos posibles, a partir de sensores remotos transportados tanto en avión, como en satélite, las cuales podrían afrontar el gran desafío de hacer la cartografía de la recarga a escalas grandes. Los métodos se

Received: 25 September 2006 / Accepted: 9 October 2006
Published online: 3 November 2006

© Springer-Verlag 2006

D. Entekhabi (✉)
Ralph M. Parsons Laboratory, Department of Civil
and Environmental Engineering, 48-331,
Massachusetts Institute of Technology,
Cambridge, MA 02139, USA
e-mail: darae@mit.edu
Tel.: +1-617-253-9698

M. Moghaddam
Radiation Laboratory,
The University of Michigan,
Ann Arbor, MI 48109-2221, USA
e-mail: mmoghadd@umich.edu

basan en sensores remotos de microonda, para medir las condiciones de superficie del terreno, en la presencia de atmósfera y de la cubierta de vegetación, que atenúan y perturban la señal, mientras ella viaja desde la superficie hacia el sensor. El énfasis está en sistemas de radar que también tienen características favorables de resolución espacial terrestre. Finalmente se presentan ejemplos de dos sistemas satelitales candidatos, como acercamientos factibles a las mediciones requeridas.

Keywords Groundwater recharge · Remote sensing · Inverse modeling · Data assimilation

Introduction

Precipitation incident at the surface and stream discharge out of watersheds are hydrological fluxes that each have a long history of monitoring. Their observations are really the only major constraints in modeling the transfers of water and biogeochemical constituents in the environment. There are, however, two other linked fluxes—evaporation and (diffuse) recharge—that play key roles in the dynamics of water transfer and storage in terrestrial environments. Evaporation and recharge are fluxes that:

- Are primary determinants of biogeochemical cycles
- Link the slow and fast components of the water cycle
- Primarily determine and are determined by vegetation distribution
- Limit the rate of sustainable use of surface waters and aquifers
- Have already dramatically changed in response to human activity

Yet there are no monitoring networks that can provide direct measurements of recharge with enough sampling to allow useful mapping (see *Hydrogeology Journal* 2002, Vol. 10, No. 1, theme issue: groundwater recharge). Direct measurement of recharge can be made using lysimeters, seepage-meters, and chemical tracers. The first two methods yield point measurements that may not be characteristic of large-scale conditions. Installation of networks of these instruments for mapping is not practical. The chemical tracer method can yield recharge estimates for effective large areas. Its limitation is that this direct measurement technique is labor-intensive and can only be performed experimentally. The approach cannot be scaled to provide large-scale mapping and global estimates.

Indirect methods for the estimation of recharge rely on linking recharge to other measurements—e.g., precipitation, stream discharge, etc.—through the use of models. Traditionally, recharge has been estimated indirectly as residual of surface or subsurface water balance. Estimates of recharge using residual techniques cannot separate model structural and parameters errors, observation errors, and any other closure errors from the identified flux values (Zhang and Schilling 2006). Lack of capability to develop

spatial mapping is also another limitation in the current suite of approaches to monitor recharge.

Evaporation and recharge are closely coupled and they depend significantly on the state of the land surface water budget. The soil moisture profile in the top few centimeters to meters of soil plays a key role in determining the rate of evaporation (including transpiration by plants) and recharge. If the soil moisture profile can be monitored on: (1) spatial scales that correspond to the scales of variation in vegetation patches and soil texture heterogeneity, and (2) temporal scales that correspond to the scales of variations in precipitation wetting and dry-down events, then a significant constraint on the estimation of evaporation and recharge will be at hand. Either time-differencing or estimation through constraining models with observations (data assimilation) can be used to map evaporation and recharge. In order to separate the two quantities, the traditional hydrologic measurements of precipitation and stream discharge can be engaged.

The above-referenced spatial and temporal scales, i.e., scales of variation in vegetation patches and soil texture heterogeneity and the scales of variations in precipitation wetting and dry-down events, themselves elude simple definitions because they depend on environmental factors that vary widely. Spatial heterogeneity and temporal intermittency exist over a wide range of spectra. Yet at the end, it is the application that sets the limit on the useful part of the spectrum that contributes relevant variability. For the current and foreseeable range of applications in water resources (monitoring surface water bodies, aquifer recharge and discharge), in regional biogeochemical budgets, in operational numerical weather prediction (model initializations), in flood forecasting, and in drought hazards mitigation, the relevant spatial and temporal scales of variations can be on the order of several hundred meters to several kilometers (order 0.1–10 km) and 1–3 days. Deeper soil moisture has damped temporal variability and 7–10 day sampling may be adequate. To remotely sense the soil moisture profile with these measurement requirements necessitates the use of microwave radar instruments. Simultaneous passive monitoring instruments or radiometers also provide useful constraints for geophysical interpretation of the signals measured by the radar instruments.

Jackson (2002) provides a review of the evolution and historical focusing of the approaches towards remote sensing of soil moisture with emphasis on recharge estimation. A brief review has again been undertaken for this paper on the advantages of microwave remote sensing for monitoring soil moisture profiles but focusing on candidate technological approaches to achieve the goals in order to build on Jackson (2002). This paper offers technological roadmaps for addressing the need for mapping recharge fields. An outline is provided of two sample spaceborne mission concepts that are technologically feasible and represent possible (complementary) paths forward. Also demonstrated, is the capability to infer recharge flux from soil moisture state observations using data assimilation.

Microwave sensing of surface and subsurface

Electromagnetic radiation in the microwave regime, which extends from about 100 MHz to about 30 GHz, has been widely used in remote sensing of the Earth's land surface environment from airborne and spaceborne platforms (see Table 1). One reason is that microwave measurements are largely unaffected by the presence of clouds, and, up to wavelengths of about 3 cm, are also unaffected by rain. At and below a free-space wavelength of 10 cm (3 GHz), for example, total atmospheric opacity is less than 2% in the presence of heavy water clouds and less than 5% in the presence of heavy rain (Ulaby et al. 1981). Atmospheric medium opacity decreases as the frequency decreases. Furthermore, microwave sensors do not depend on solar radiation as the source of target illumination.

Microwave radiometers, which are passive sensors that only act as receivers, measure the emitted radiation (characterized as brightness temperature) of targets (Njoku and Entekhabi 1996). On the other hand, radars including altimeters, scatterometers, and synthetic aperture radars (SARs), measure the backscattering cross section of targets due to the active microwave transmission source provided by the sensor itself (Ulaby et al. 1996).

Both radiometers and radars are primarily sensitive to the dielectric properties of the targets present in the scene. Dielectric constants of objects and media in turn are strong functions of their water content. The relationship between dielectric constant and soil moisture, for example, has been studied extensively and determined for various frequencies and soil textures (e.g., Dobson et al. 1985; Peplinski et al. 1995). Likewise, the dielectric constant of vegetation has been shown to be a strong function of its moisture content (Ulaby et al. 1996). The specific form in which the microwave measurements are related to dielectric constant of soil and vegetation can be studied via a number of radiative transfer or electromagnetic scattering models. In general, radiometric measurements of brightness temperature (a measure of emitted radiation in the microwave spectral range) have been shown to be less sensitive than radar to geometric parameters of the scene such as soil surface roughness or vegetation structural properties, which helps constrain the variations in a given measurement to those of the moisture content alone. On the other hand, radars are quite sensitive to these geometric parameters in addition to the dielectric

constant, which could be considered a strength in that it is possible to design measurement parameters to optimize the data information content for both moisture and geometric properties.

Although microwaves are quite insensitive to clouds and rain as they propagate through the atmosphere, they can be severely attenuated by conductive and dielectric losses of soil and vegetation. For higher microwave frequencies, the rate of attenuation is higher, as shown in Fig. 1, for some sample microwave bands. For a given frequency, attenuation rate increases for denser vegetation or increased moisture content in soil or vegetation. At L-band (24 cm), for example, the presence of 5 kg/m² of vegetation and more attenuates the signal such that the sensitivity to surface soil moisture variations is reduced. Some sample calculations of attenuation will follow shortly. It must be noted that microwaves at L-band and lower are prone to adverse ionospheric impacts such as scintillation and Faraday rotation if operated from a spaceborne platform, in which case proper mitigation strategies must be employed.

To penetrate vegetation, soil surface, and deep soil, lower-frequency microwaves are needed due to their ability to travel through significant vegetation canopies and through soil with a low attenuation rate and, therefore, without losing needed information content. Although passive microwaves at frequencies above 1 GHz have been widely used in several past, present, and planned radiometer systems, they are best for retrieving surface soil moisture in no- or low-vegetation areas (Nichols et al. 1993; Jackson et al. 1999; Jackson and Schmugge 1991). Furthermore, in the presence of vegetation and to penetrate into deeper soil, a radar is needed to achieve the required resolutions at lower frequencies with reason-

Table 1 Microwave letter band nomenclature

Name	Frequency (GHz)	Wavelength in free space (cm)
VHF	0.05–0.15	600–200
P	0.230–1.0	130–30
UHF	0.43–1.3	70–23
L	1.0–2.0	30.0–15.0
S	2.0–4.0	15.0–7.5
C	4.0–8.0	7.5–3.8
X	8.0–12	3.8–2.5
Ku	12–18	2.5–1.7
K	18–27	1.7–1.1
Ka	27–40	1.1–0.75

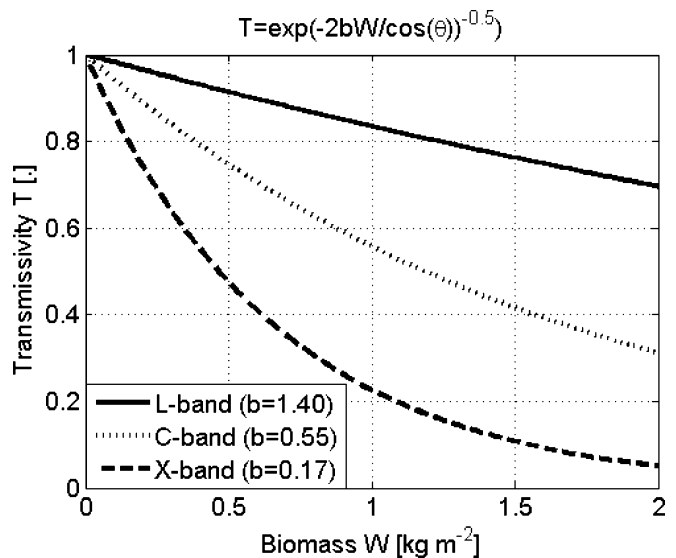


Fig. 1 Canopy transmissivity (complement of opacity) for sample microwave bands (horizontal co-polarization at 20° incident angle). Increasing biomass density reduces the transmissivity across the canopy. The effect is less pronounced at lower microwave frequencies (based on parameters found in Ulaby et al. 1996 and Jackson and Schmugge 1991)

able antenna sizes. Real-aperture antenna radiometers would require prohibitively large antennas at frequencies below about 1 GHz, and hence are not considered suitable candidates for lower-frequency applications.

Figure 2 shows the expected depth of sensitivity of reflected microwaves (i.e., penetration depths) from soil at three representative frequencies in the L-band, UHF, and VHF ranges. It is observed that the one-way penetration depth could reach tens of centimeters to several meters depending on the moisture content and soil type. The penetration depth is defined as the distance over which the wave amplitude decays to $1/e$ (-8.7 dB or decibel) of its original value. Here, attenuation due to soil moisture is considered. Additionally, soil texture variations, rock inclusions and other structural soil factors may be present. From an electromagnetic propagation point of view, at any given frequency, the loss tangent of the soil medium, i.e., the ratio of the imaginary to real parts of the dielectric constant, is the determinant of the loss encountered by the waves as they travel through the medium and is a function of soil texture and moisture content. For the same soil type and frequency, higher moisture content results in higher loss tangent and, therefore, smaller depth of penetration.

An example of the use of a radar system for subcanopy soil moisture estimation is given in Fig. 3 (Moghaddam et al. 2000), where it has been shown that moisture variations of soil under a 15-m tall boreal forest canopy and down to a soil depth of about 0.5–1 m can be

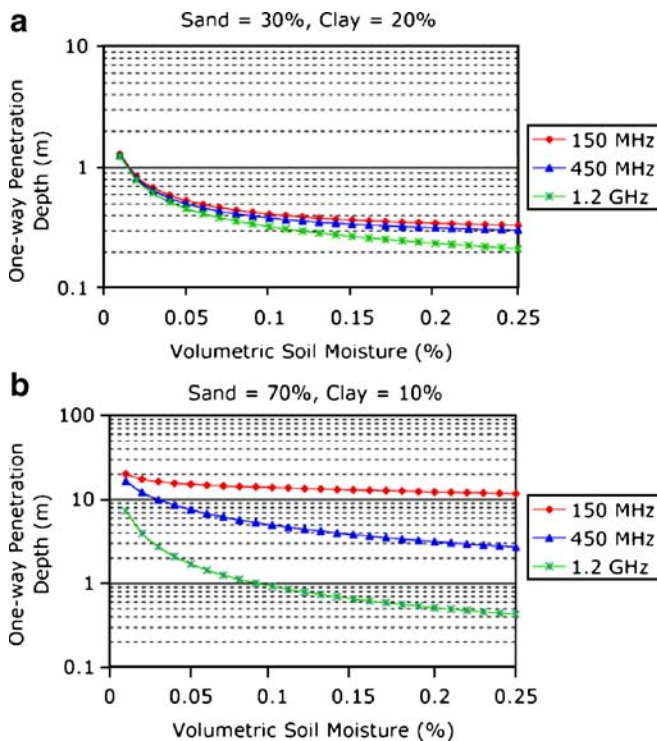


Fig. 2 Penetration depth as a function of soil moisture for two different soil types **a** 30% sand, 20% clay, and **b** 70% sand, 10% clay. Penetration depth increases from L-band (1.2 GHz) to UHF (450 MHz) to VHF (150 MHz). Standard plane wave-propagation models and the soil dielectric model of Peplinski et al. (1995) and Dobson et al. (1985) are used

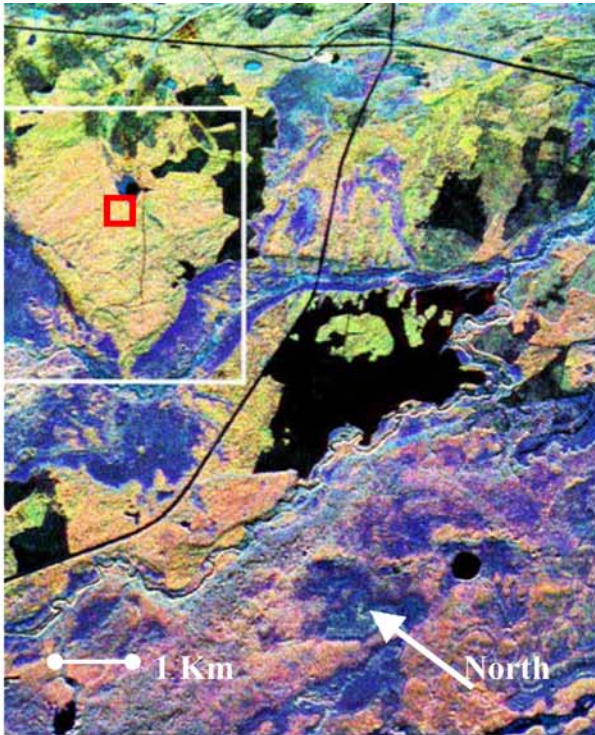
Fig. 3 **a** RGB (red-green-blue) color-coded overlay of P/L/C frequency AIRSAR (AIRborne Synthetic Aperture Radar) image in a boreal forest region in Saskatchewan, Canada. **b** Comparison of estimated and measured subcanopy soil moisture for the red box in part **a**. Due to possible calibration errors, all values are underestimated, with better than 1% accuracy if the bias is removed after differencing. **c** Stand-wide estimates of soil moisture for the white box in part **a** (June to September 1994), with black-to-red-to-yellow-to-white color range representing 0–10% gravimetric soil moisture scale

estimated to 3–4% absolute and 1% change accuracy using L- and P-band radar data. The canopy closure is 60%, and the biomass is about 11 kg/m². For forests of higher closure and deeper crown layer (larger biomass), lower frequencies will be required to achieve higher sensitivity to soil moisture, as shown in Fig. 4.

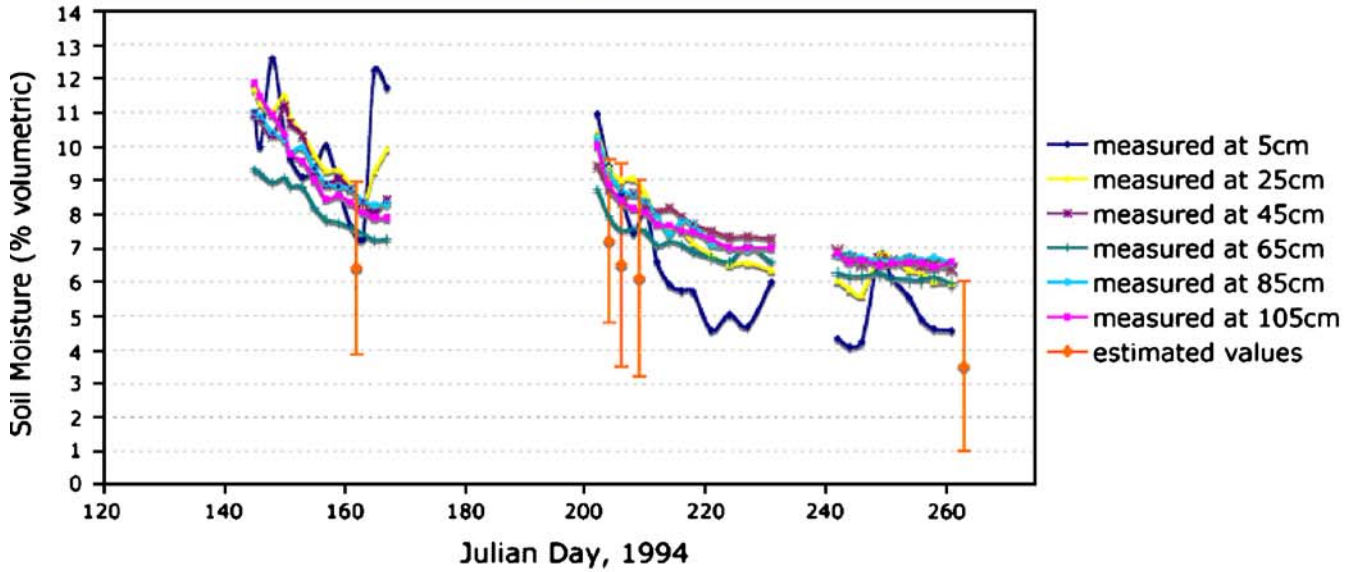
Ideally, three observation frequencies could be used (L-band, UHF, and VHF). The L-band frequency can be used to estimate soil moisture in the top 0–5 cm in the presence of up to 5 kg/m² of vegetation (Dubois et al. 1995; Oh et al. 1992). P-band measurements are needed to (1) enhance capability to characterize vegetation effects as the amount of vegetation is increased to up to 20 kg/m² (Dobson et al. 1992; Freeman et al. 1992; Rignot et al. 1995), and (2) retrieve soil moisture in the 0–50 cm depth, depending on the amount of soil moisture present (Moghaddam et al. 2000).

Having both L- and P-band data enables a more complete characterization of the various layers of a vegetation canopy if such information is needed. The VHF data are indispensable for retrieving soil moisture under vegetation canopies exceeding 20 kg/m² and to depths of 2 m or more, depending on the amount of moisture present. However, at least one of the higher frequencies, preferably P-band, must be present for separating, characterizing, and removing the contribution of the vegetation layer. Fully polarimetric measurements are needed at all frequencies for canopy characterization as well as removal of ionospheric effects in the case of a spaceborne system.

A major constraint in making radiometric measurements at GHz and sub-GHz frequencies is the requirement for large-size antennas. The ground resolution of the measurement is inversely proportional to the height of the instrument above the target and directly proportional to the spectral frequency. At low Earth orbit (~500–2,000 km) the antenna reflector needs to be several meters to tens of meters in diameter for a radiometer to achieve the required resolutions of O(10 km). Although the size of the antenna for a synthetic aperture radar (SAR) does not grow with wavelength, the temporal sampling requirements for soil moisture mandate that a large antenna be used for these instruments. For example, to achieve a weekly repeat observation of the globe, swath widths of approximately 400 km are needed, which in turn translate into SAR antenna lengths of 30 m or larger, regardless of frequency. Large deployable and lightweight antenna reflectors have been developed for space telecommunications. These reflectors perform well at the needed microwave frequency ranges and they can be stowed for



P-band **L-band** **C-band**



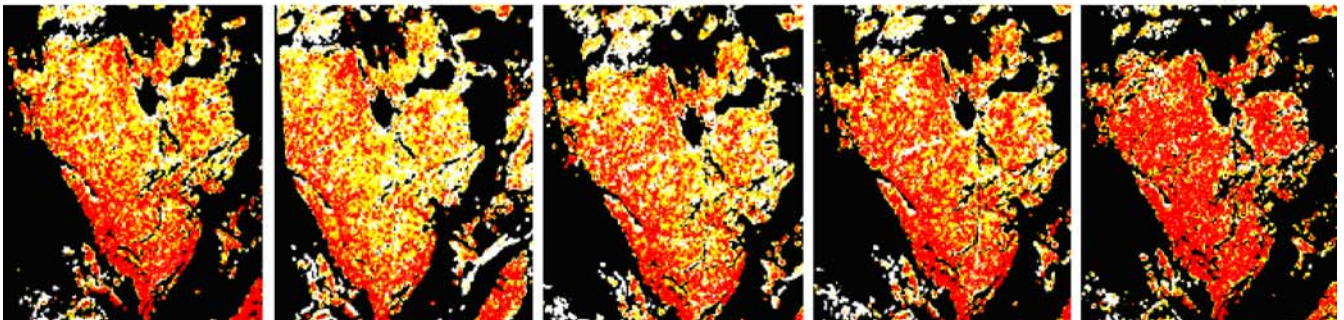
6/11/94

7/23/94

7/25/94

7/28/94

9/20/94



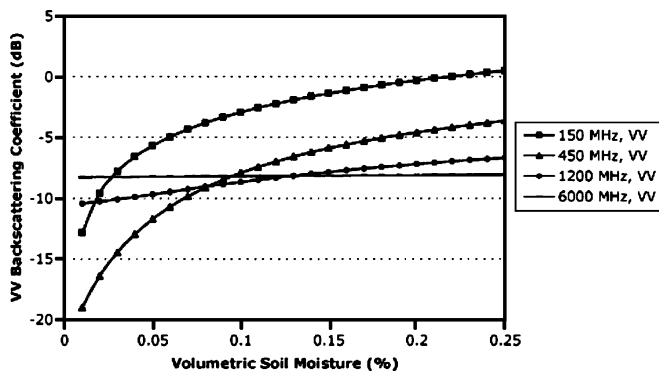


Fig. 4 Dependence of radar backscattering coefficient (in decibels) to soil moisture under forest canopy for frequencies ranging from C-band (6 GHz shown here) to VHF (150 MHz shown here). The forest is assumed to have 200 tons/ha of vegetation. Sensitivity to soil moisture decreases substantially for L-band and higher. Forest scattering model of Durden et al. (1989) is used to generate these data, along with the soil dielectric model of Peplinski et al. (1995) and Dobson et al. (1985). *VV* vertical transmit–vertical receive polarization

launch and then deployed. There is considerable use of such antennas for telecommunications and they now have significant space environment heritage. As candidate mission concepts that meet the measurement requirements, two examples are briefly presented. Both concepts have been studied for technical feasibility and their performance has been tested with numerical or theoretical tools as well as scale models. Both MOSS and Hydros are mission concepts and not programs in implementation at this time.

The MOSS concept has a larger antenna and can measure P-band as well as VHF backscattering cross sections. It is, in principle, also possible to add an L-band radar or radiometer system. Its design is to make measurements in a side-looking fashion. The spacecraft and antenna orbit the Earth and make measurements along the satellite ground track, allowing complete global mapping every 7–10 days. With the lower frequency, the deeper subsurface or soil moisture profile may be monitored globally. This is consistent with the requirements for deeper soil-moisture measurements.

The Hydros concept has a smaller antenna and can be rotated along its vertical axis to make conical scans of the surface across a wide swath. Its size limits it to L-band but the wide swath of measurements of the surface soil moisture allows a measurement refresh or sampling every 2–3 days. This is consistent with the requirement for surface soil-moisture measurement.

MOSS mission concept

Microwave observatory of subcanopy and subsurface (MOSS) is a synthetic-aperture radar (SAR) Earth-orbiting system under conceptual and technology development as part of the NASA (National Aeronautics and Space Administration) Earth-Sun System Science Technology Office Instrument Incubator Program (IIP) for global

observations of soil moisture under substantial vegetation canopies and at depths of down to several meters (Moghaddam et al. 2005, personal observations, 2006). It consists of an SAR operating at two low frequencies simultaneously, one in the UHF and the other in the VHF range. Observations at these low frequencies allow the estimation of soil moisture in the decimeter-to-meters range below the surface, and in the presence of substantial vegetation canopies. The measurements are fully polarimetric and system parameters are chosen to allow resolutions of 1 km or better, even with averaging more than 100 looks. To demonstrate the depth of penetration of such a radar system and corroborate the theoretical results shown in Figs. 2 and 4, the authors developed a tower-based radar, operating at the same VHF and UHF frequencies, and deployed it in Arizona (bare surface) and Oregon (forested), USA. In situ soil moisture probes were installed for validation of radar estimation results. In Arizona, the soil moisture profile was successfully retrieved and validated to a depth of 2 m, which was the location of the deepest probe. The worst-case absolute estimation error was 7% (Moghaddam et al. , personal observations, 2006). The radar image was formed for larger depths as well, but due to lack of in situ sensors, it could not be directly validated. In Oregon, likewise, radar images were successfully formed to a subsurface depth of 60 cm (location of bedrock) in the presence of a 15–20 m tall dense conifer stand. Initial soil moisture profile estimates have been derived, with further analysis and currently underway for this data set.

Several technological challenges for the implementation of the MOSS spaceborne mission have been studied and their solutions matured. These include the design of a large aperture antenna and prototyping of its feed system, frequency interference analyses, and correction of ionospheric effects. The required repeat observation period of 7–10 days imposes a requirement on the instrument's swath width and hence the antenna size. Specifically, for an 8-day repeat observation period, both frequencies require an antenna length of 30 m, while each requires a

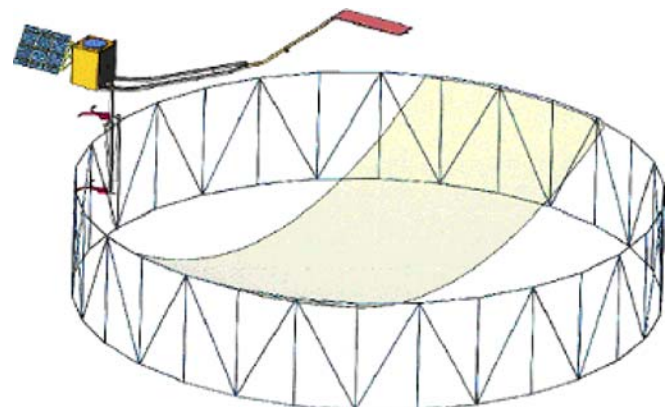


Fig. 5 MOSS proposed spacecraft-antenna configuration, showing the subillumination of the 30 m-diameter-mesh-reflector antenna by the dual-frequency feed system

different antenna width (11 m at VHF, 3 m at UHF). Using conventional phased-array technologies, the two antennas, even with a shared-aperture architecture, would have a mass in excess of 4,000 kg, rendering the mission unfeasible. The concept proposed by MOSS was to synthesize the two different antenna widths on a single parabolic mesh reflector of 30-m diameter (Fig. 5) by subilluminating the reflector surface with a dual-frequency stacked patch-microstrip-array feed. The resulting total antenna system mass is one order of magnitude lower than the conventional approach, while carrying significantly lower risk than other antenna concepts such as inflatables. MOSS has prototyped this antenna feed system to show the feasibility of the overall concept.

The mission scenario for MOSS is achieved from a sun-synchronous orbit of 1,313 km altitude, with a swath width of 340–430 km, incidence angle ranges of 17–30°, resolution of 1 km, and an 8-day exact repeat consistent with the temporal scale of variations of the subcanopy and subsurface soil moisture. Complementary to proposed soil moisture missions at L-band, which aim at retrieving the top surface soil moisture for low- or no-vegetation areas at 3-day sampling intervals, this mission optimizes the system design for under-vegetation and deep soil moisture, in addition to simultaneous measurement of the soil moisture at the top few centimeters.

Hydros mission concept

The Hydrosphere State (Hydros) mission concept was developed in response to a call for proposed exploratory Earth missions under the NASA Earth Systems Science Pathfinder (ESSP) program in 2001. Entekhabi et al. (2004) gives detailed descriptions of the science goals and baseline design. Hydros design uses a combined radiometer and radar L-band microwave instruments to measure the land hydrosphere state globally from space. The measurements allow estimation of surface soil moisture (0–5 cm depth) and land freeze/thaw state over a wide 1,000-km swath with a global revisit of 2–3 days (1–2 days above 50° latitude). Over 70% of the swath, the radar resolution is better than 3 km. The radiometer resolution is about 40 km. Measurements from these sensors are combined to produce a global 10-km soil-moisture data product.

The radar and the radiometer share the aperture of a large (6 m) but lightweight deployable mesh reflector (see Fig. 6). The reflector rotates to make conical scans over a wide swath (~1,000 km). In this way Hydros will produce global mapping with high revisit.

The spatial resolution of the radiometer measurements are determined by the dimensions of the antenna beam “footprint” projected on the Earth’s surface. To obtain the required high-resolution radar data, range and Doppler discrimination will be employed. This is equivalent to the application of SAR techniques to the conically scanning radar case. Due to squint angle effects, the high-resolution products will not be obtained within a narrow swath band

centered on the spacecraft nadir track in the direction of orbital travel. The unique aspect of the Hydros application is the necessity for rotating the antenna. At an altitude of 670 km, the reflector must be rotated at a rate of 14.6 rpm to maintain contiguity (i.e., minimum overlap) of the measurements in the along-track direction.

There is a unique opportunity to sample the radiometric capability of Hydros with a forthcoming mission. The European Space Agency’s Soil Moisture and Ocean Salinity (SMOS) mission is due for launch in 2007 (Kerr et al. 2001). SMOS has a two-dimensional synthetic aperture antenna that make measurements of surface passively emitted radiation at L-band (polarimetric). The sensitivity is excellent and the orbit and revisit characteristics are similar to those mentioned for Hydros above. SMOS is a radiometer-only mission and its measurements are at about 40–50-km ground resolution. Hydros design additionally includes a radar for higher resolution but the forthcoming SMOS data are highly valuable for demonstrations and refinements of science and operational applications.

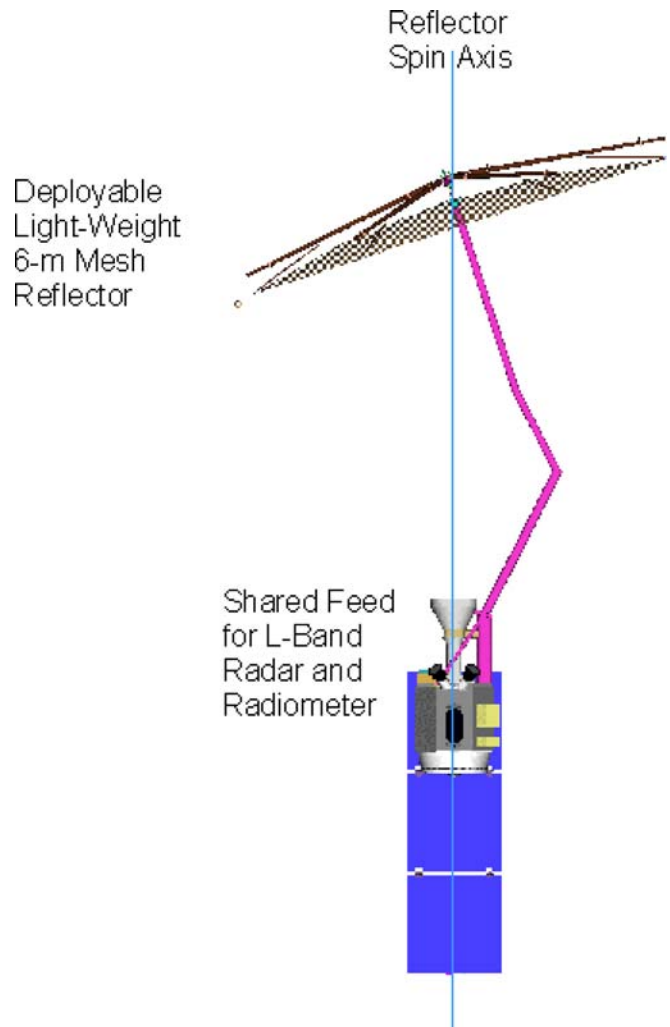


Fig. 6 Hydros proposed spacecraft-antenna configuration with a 6-m-diameter mesh reflector for shared radar and radiometer sensors

Opportunity for a combined mission

With substantial advances made and more analysis underway for both Hydros and MOSS mission concepts and science products, it could be plausible to combine the two measurements for an integrated view of soil moisture profiles, from surface to depth, and for a large range of vegetation conditions. A prospective mission like this would span the frequency decade 0.14–1.4 GHz, for a next-generation soil moisture mission, and could enable a *comprehensive soil-moisture solution*:

- At multiple columns, starting from surface to depths of several meters
- Under substantial vegetation canopies exceeding 20 kg/m² water content
- At 3-day intervals

The spatial resolution will be 1 km for the synthetic aperture radar (SAR) instruments and 20 km for the radiometer. The specific antenna technology to be adopted for such a mission will require an in-depth study to consider feasibility and performance trade-offs.

From soil-moisture profile measurements to recharge estimation

The Hydros and MOSS concepts provide measurements of soil moisture state, i.e., the volumetric soil moisture content, through sensing the dielectric constant of the soil. The estimation of recharge flux from these state measurements can be achieved through various schemes. There is extensive literature on various approaches to infer diffuse recharge from soil-moisture profile observations (e.g., Rushton and Ward 1979; Sophocleous and Perry 1984; Sophocleous 1991; Allison et al. 1994; Finch 1998; Scott et al. 2000; Rushton et al. 2006). Most of these techniques use mass balance, Darcy equation, or zero-flux plane techniques (Scanlon et al. 2002). The quality of the estimates does depend on the vertical resolution of the measurement and temporal sampling.

An alternate approach is to use the available state observations to constrain a physics-based dynamic model. This is known as data assimilation and it is distinct from model calibration because both model forecasts and observations are considered uncertain. In land data, assimilation measurements are used to update the states of the model whenever they are available. Again, it is assumed that both the measurements and the model forecasts are prone to error. Estimates of these errors are propagated in time just as the state. At the time of measurements, the propagated uncertainty levels are used to develop an estimate of model state conditioned on measurements using Bayesian probability concepts. The merged estimates are considered to be statistically optimal since they minimize an appropriate-

ly defined model-observations misfit cost function. There are a number of different data assimilation techniques each with advantages and disadvantages relative to the problem. Examples of data assimilation for the purposes of soil-moisture-profile estimation using remote sensing observations can be found in Galantowicz et al. (1999) and Walker et al. (2001). Margulis et al. (2002), Reichle et al. (2002), Crow and Wood (2003), Dunne and Entekhabi (2005), among others, have adapted the ensemble Kalman filter (EnKF) that is a sequential data assimilation framework. The EnKF has been shown to be particularly suitable for land surface problems because of its flexibility in dealing with: (1) multiplicative as well as additive model errors, i.e., errors in parameters and boundary conditions, and (2) nonlinear dynamic propagation of model states. In this work, an Observing System Simulation Experiment (OSSE) was implemented based on a basic one-dimensional EnKF to represent a characteristic measurement pixel. The truth is a single “open-loop” replicate from an ensemble with N_{rep} members, i.e., unconstrained by observations, integration of the soil model with micrometeorological surface boundary and open drainage lower boundary conditions. Observations are sampled from the truth and noise (Gaussian with covariance R) added to replicate measurement error. The soil-moisture profile dynamics center-difference solver here has 50 nodes extending to 2.5 m below the surface and it is implemented with implicit time scheme and explicit linearization of Brooks-Corey soil hydraulic properties (soil saturated hydraulic conductivity, saturation matric head, pore-size distribution index, and porosity respectively are: $K_{\text{sat}}=1.7 \times 10^{-7}$ m/s, $\psi(1)=-0.35$ m, $m=1.3$, and $n=0.35$).

The principal source of uncertainty in the model is precipitation. In this example, different synthetic traces of precipitation are used to create an ensemble of uncertain forecasts. The precipitation traces are generated using a rectangular pulses model (see Eagleson 1978) with identical parameters (mean time between storms, mean storm duration, and mean storm intensity are: $m_{t_b} = 120$ hours, $m_{t_r} = 4$ hours, and $m_{i_r} = 4$ mm/hr, respectively) ensuring long-term hydroclimate consistency. The soil is subject to transpiration-root-water extraction, here modeled with exponentially decaying root distribution (e -folding depth of 25 cm) and a diurnally varying potential evaporation peaking at 4.8 mm/day. Soil water deficit reduces actual evapotranspiration according to the classic functional form defined by Deardorff (1978).

The errors in model forecasts are principally due to the uncertainty in precipitation. This error enters the system through the boundary condition and in a non-linear fashion. The EnKF ensemble of equally likely replicates (state vector y_t^j where $j=1, \dots, N_{\text{rep}}$) are propagated forward in time (t) using the full solver. At the time of measurements availability (taken to be once every 3 days in this case), the ensemble sample covariances C_{yz} and C_{zz} are used to produce an updated state vector y_t^j based on the (perturbed) observations Z and forecasts y_t^j . The (Kalman)

Fig. 7 Soil moisture volumetric content (θ) dynamics in two sections of the profile: **a** 0–5 cm and **b** the uppermost meter. The synthetic truth (red line with circles) is characterized by storm and dry-down events. The open-loop ensemble mean (*Ens. Mean*) and bracketing one standard deviation (*blue lines*) are also shown

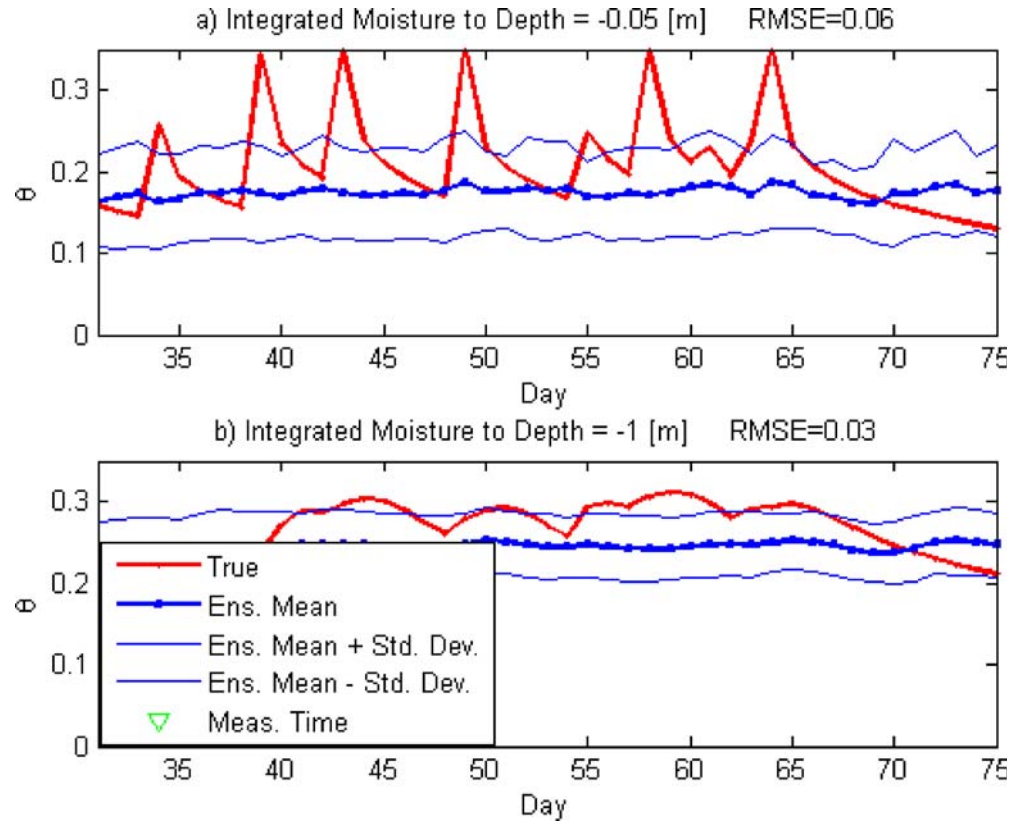


Fig. 8 Recharge (normalized by the soil saturated hydraulic conductivity K_{sat}) across **a** the 75 cm and **b** 125-cm planes below the surface. See Fig. 7 for legend

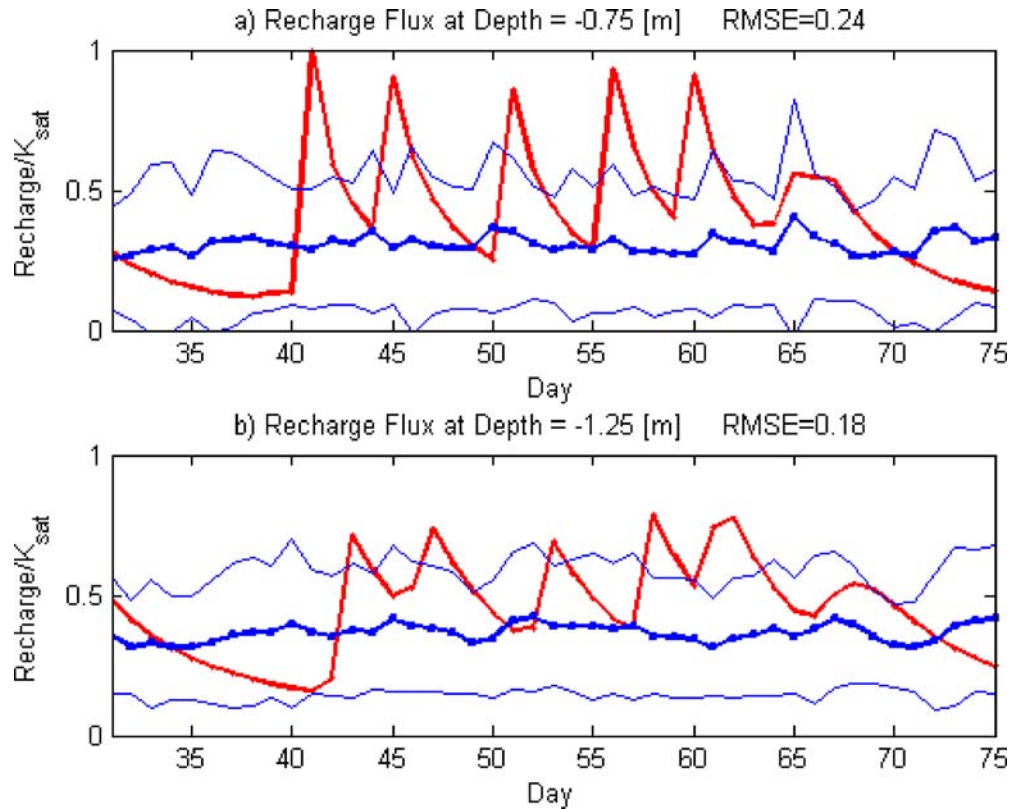


Fig. 9 Recharge (normalized by K_{sat}) across **a** the 75 cm and **b** 125-cm planes below the surface with L-band measurements (timing noted as *green triangles on abscissa*). See Fig. 7 for legend

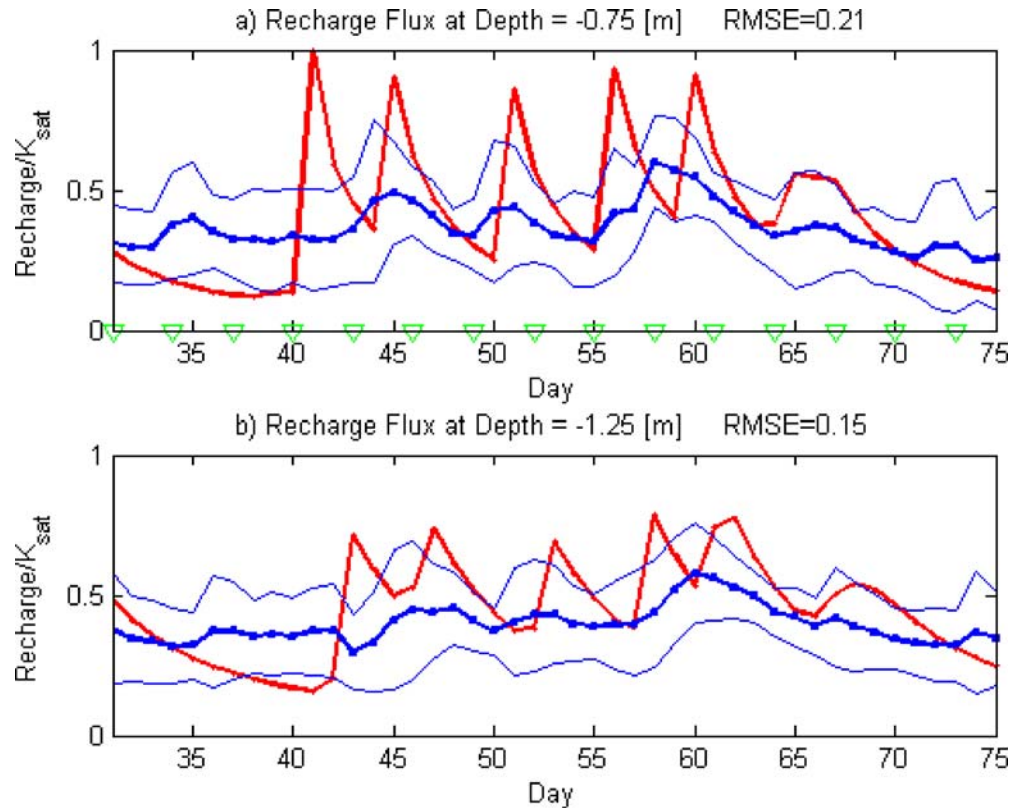
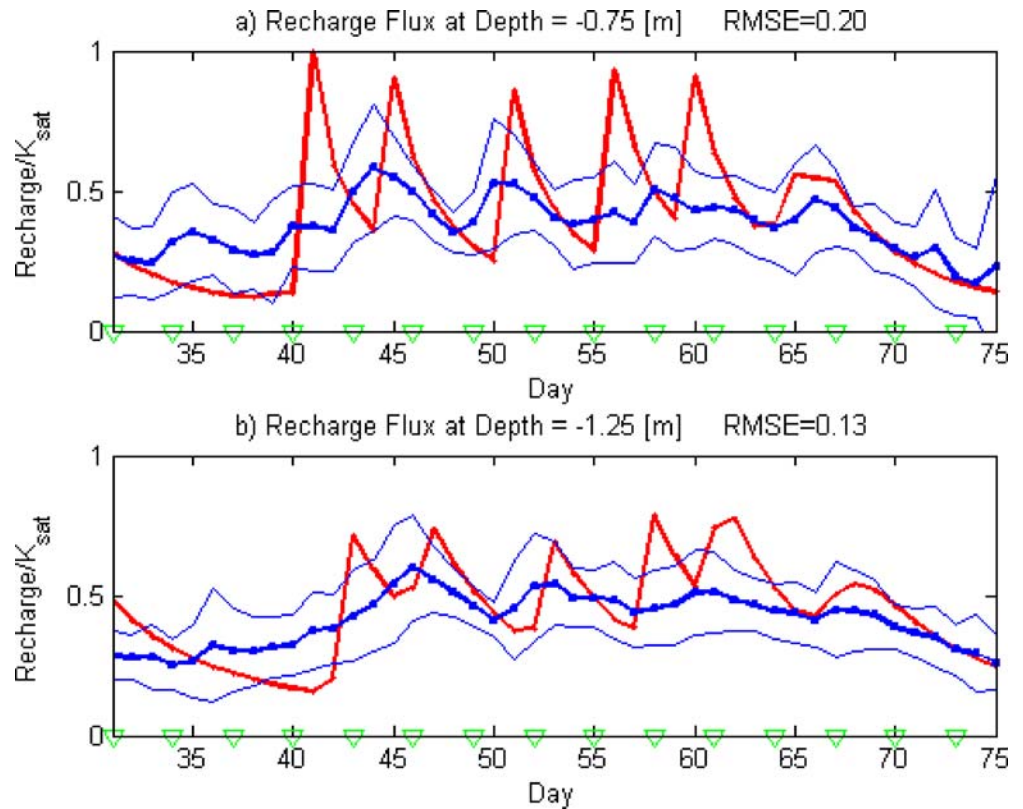


Fig. 10 Recharge (normalized by K_{sat}) across **a** the 75 cm and **b** 125 cm planes below the surface both with L-band and P-band measurements (timing noted as *green triangles on abscissa*). See Fig. 7 for legend



update that minimizes the posterior covariance of the estimate is

$$y_t^j = y_t^j + C_{yy}(C_{zz} + R)^{-1}(Z - M \cdot y_t^j) \quad (1)$$

Here M is a matrix that projects the states onto observations space. In the case of both L- and P-band observations, it is a non-square matrix that averages the soil moisture within the top 5 cm and to 100 cm. In a more sophisticated implementation of EnKF, the M could be a non-linear operator that includes the forward back-scatter models and can therefore deal with moisture-dependent sensing depth (see Fig. 2). The matrix $C_{yy}(C_{zz}+R)^{-1}$ is the projection of observations misfits onto the state update increments.

In this demonstration application, a period with a few storms and dry-down events is selected. Three cases are considered: (1) “open-loop” where no remote sensing information is available, (2) when only L-band measurement is available, and (3) when the synergy of L- and P-band measurements with different penetration sensing depths are available.

Figure 7 shows the open-loop time-series of the state over the OSSE period. Figure 7a shows the top 5-cm soil moisture and Fig. 7b shows the top meter average volumetric soil-moisture content. The observations (red line with circles) show several precipitation events and dry downs for the synthetic truth. The open-loop ensemble mean represents the average of many replicates with precipitation uncertainty (thick blue line with squares; thin blue lines are plus and minus one standard deviation). The values represent the general hydroclimate of the case. There are no soil-moisture state observations to correct the ensemble towards the measurements of the truth. The root mean squared deviation (RMSE) with respect to the withheld truth is 5.9% volumetric soil water content for the top 5 cm and 2.9% for the top meter (lower dynamic range in general). Calculated RMSE values are reported on the figures. When L-band observations are available, the state ensemble mean gravitates towards the measurement, especially for the top 5-cm case (not shown; RMSE of top 5 cm is reduced to 3.7% and the RMSE of top meter is 2.0% since the information from the surface does eventually reach the depths beyond the sensor sensitivity). When P-band measurements are added, the RMSE of the top 5 cm does not change but, as expected, the RMSE of the top meter average volumetric water content is reduced to 1.6%, nearly half of the open-loop case (time-series not shown). What is important is the capability to infer recharge at depth from the data assimilation framework.

Figures 8, 9 and 10 show the recharge time-series for the three cases: “open-loop”, L-band only, and L- and P-band, respectively. The plotted recharge values are normalized by K_{sat} and are thus non-dimensional. The expectation is that the inclusion of L-band improves over the open-loop especially near the surface. When P-band is

additionally included, the recharge at depth should be better estimated. Figure 8 represents the time-series of the open-loop with the same color notation as Fig. 7. The green symbols on the abscissa represent the discrete and intermittent measurement times. Recharge values are calculated as flux across the plane at 75 cm below the surface (in Figs. 8a, 9a and 10a) and 125 cm below the surface (in Figs. 8b, 9b and 10b) as examples.

Figure 8 results show the open-loop ensemble mean and bracketing (one) standard deviations as characteristic of climatological value since there are no observation constraints to add information. The truth (red line with circles) shows precipitation episodes with infiltration and diffusion fronts that reach depths with damped and delayed dynamics. When L-band measurements are added (Fig. 9), the errors in estimation are reduced, especially close to the surface. The ensemble mean reflects the dynamics of the true storm and dry-down events to a limited degree. When the P-band measurements are added to the L-band (Fig. 10), the recharge estimates are still improved especially at the deeper (–125 cm) level. Furthermore the error of estimation, i.e., the ensemble spread measured by the standard deviations, is reduced for recharge at both depths, indicating enhanced robustness of estimation with the inclusion of the added measurement.

This one-dimensional EnKF-based OSSE is meant to demonstrate a feasible path forward for using Hydros- and MOSS-type measurements of soil moisture state to estimate diffuse recharge flux at depths in the soil column. The framework is particularly useful to perform trade-offs on measurement accuracy, revisit and other instrument and mission parameters. These trade-offs are critical to the formulation phase refinement of the missions.

Summary

In this paper, the motivation for using microwave remote sensing-especially spaceborne radars operating at GHz and sub-GHz frequency ranges-is presented. The goal is to allow more direct measurements of factors that allow the mapping of recharge and evaporation fields over the terrestrial landscape. This paper follows Jackson (2002) and offers some technological and data-interpretation roadmaps for achieving the science and application goals. Candidate approaches are outlined and data assimilation techniques for inferring recharge from soil moisture profile estimates are also demonstrated.

References

- Allison GB, Gee GW, Tyler SW (1994) Vadose zone techniques for estimating ground-water recharge in arid and semiarid regions. *Soil Sci Soc Am J* 58(1):6–14
- Crow WT, Wood EF (2003) The assimilation of remotely-sensed soil brightness temperature imagery into a land surface model using ensemble Kalman filtering: a case study based on ESTAR measurements during SGP97. *Adv Water Resour* 26(2):137–149

- Deardorff JW (1978) Efficient prediction of ground surface temperature and moisture with inclusion of a layer of vegetation. *J Geophys Res* 83:1889–1903
- Dobson MC et al (1992) Dependence of radar backscatter on conifer forest biomass. *IEEE Trans Geosci Remote Sens* 30:412–415
- Dobson MC, Ulaby FT, Hallikainen MT, El-Rayes MA (1985) Microwave dielectric behavior of wet soil, part II: dielectric mixing models. *IEEE Trans Geosci Remote Sens* GRS-23:35–46
- Dubois PC, van Zyl J, Engman T (1995) Measuring soil moisture with imaging radars. *IEEE Trans Geosci Remote Sens* 33(4):915–926
- Dunne S (2006) Hydrologic data assimilation of multi-resolution microwave radiometer and radar measurements using ensemble smoothing. PhD Thesis, Department of Civil and Environmental Engineering, Massachusetts Institute of Technology, Boston
- Dunne S, Entekhabi D (2005) An ensemble-based reanalysis approach to land data assimilation. *Water Resour Res* 41(2): DOI 10.1029/2004WR003449. Cited 13 Oct 2006
- Durden SL, Zebker HA, van Zyl JJ (1989) Modeling and observation of forest radar polarization signatures. *IEEE Trans Geosci Remote Sens* 27(3):290–301
- Eagleson PS (1978) Climate, soil, and vegetation. 2. The distribution of annual precipitation derived from observed storm sequences. *Water Resour Res* 14(5):713–721
- Entekhabi D, Njoku E, Houser P, Spencer M, Doiron T, Smith J, Girard R, Belair S, Crow W, Jackson T, Kerr Y, Kimball J, Koster R, McDonald K, O'Neill P, Pultz T, Running S, Shi JC, Wood E, van Zyl J (2004) The Hydrosphere State mission concept: an Earth system pathfinder for global mapping of soil moisture and land freeze/thaw. *IEEE Trans Geosci Remote Sens* 42(10):2184–2195
- Finch JW (1998) Estimating direct groundwater recharge using a simple water balance model-sensitivity to land surface parameters. *J Hydrol* 211(1–4):112–125
- Freeman A, Durden SL, Zimmermann R (1992) Mapping subtropical vegetation using multifrequency, multipolarization SAR data. *Proc IGARSS'92*, Houston, TX, pp 1986–1689
- Galantowicz J, Entekhabi D, Njoku E (1999) Tests of sequential data assimilation for retrieving profile soil moisture and temperature from observed L-band radiobrightness. *IEEE Trans Geosci Remote Sens* 37(4):1860–1870
- Jackson TJ (2002) Remote sensing of soil moisture: implications for groundwater recharge. *Hydrogeol J* 10(1):40–51
- Jackson TJ, Schmugge TJ (1991) Vegetation effects on the microwave emission of soils. *Remote Sens Environ* 36:203–212
- Jackson TJ, Le Vine DM, Hsu AY, Oldak A, Starks PJ, Swift CT, Isham J, Haken M (1999) Soil moisture mapping at regional scales using microwave radiometry: the Southern Great Plains hydrology experiment. *IEEE Trans Geosci Remote Sens* 37:2136–2151
- Kerr YH, Waldteufel P, Wigneron JP, Martinuzzi J, Font J, Berger M (2001) Soil moisture retrieval from space: the Soil Moisture and Ocean Salinity (SMOS) mission. *IEEE Trans Geosci Remote Sens* 39(8):1729–1735
- Margulis SA, McLaughlin D, Entekhabi D, Dunne S (2002) Land data assimilation and estimation of soil moisture using measurements from the Southern Great Plains 1997 field experiment. *Water Resour Res* 38(12) DOI 10.1029/2001WR001114. Cited 13 Oct 2006
- Moghaddam M, Saatchi S, Cuenca R (2000) Estimating subcanopy soil moisture with radar. *J Geophys Res-Atmos* 105(D11):14899–14911
- Moghaddam et al (2005) Microwave Observatory of Subcanopy and Subsurface (MOSS) IIP: final results and next steps. *Proceedings of ESTC-2005*, Washington, DC, June 2005
- Nichols WE, Cuenca RH, Schmugge TJ, Wang JR (1993) Push-broom microwave radiometer results from HAPEX-MOBILHY. *Remote Sens Environ* 46(2):119–128
- Njoku EG, Entekhabi D (1996) Passive microwave remote sensing of soil moisture. *J Hydrol* 184(1–2):101–129
- Oh Y, Sarabandi K, Ulaby FT (1992) An empirical model and an inversion technique for radar scattering from bare soil surface. *IEEE Trans Geosci Remote Sens* 30(2):370–381
- Peplinski NR, Ulaby FT, Dobson MC (1995) Dielectric properties of soils in the 0.3–1.3-GHz Range. *IEEE Trans Geosci Remote Sens* 33(3):803–807 DOI 10.1175/1520-0493
- Reichle R, McLaughlin D, Entekhabi D (2002) Hydrologic data assimilation with the ensemble Kalman filter. *Mon Weather Rev* 130(1):103–114
- Rignot E, Zimmermann R, van Zyl J, Oren R (1995) Spaceborne applications of a P-band imaging Radar for mapping of forest biomass. *IEEE Trans Geosci Remote Sens* 33(5):1162–1169
- Rushton KR, Ward C (1979) The estimation of groundwater recharge. *J Hydrol* 41(3–4):345–361
- Rushton KR, Eilers VHM, Carter RC (2006) Improved soil moisture balance methodology for recharge estimation. *J Hydrol* 318(1–4):379–399
- Scanlon BR, Healy RW, Cook PG (2002) Choosing appropriate techniques for quantifying ground-water recharge. *Hydrogeol J* 10(1):18–39
- Scott RL, Shuttleworth WJ, Keefer TO, Warrick AW (2000) Modeling multi-year observations of soil moisture recharge in the semi-arid American southwest. *Water Resour Res* 36(8):2233–2247
- Sophocleous MA (1991) Combining the soil-water balance and water-level fluctuation methods to estimate natural ground-water recharge-practical aspects. *J Hydrol* 124(3–4):229–241
- Sophocleous MA, Perry CA (1984) Experimental studies in natural ground-water-recharge dynamics-assessment of recent advances in instrumentation. *J Hydrol* 70(1–4):369–382
- Ulaby F, Moore R, Fung A (1981) *Microwave remote sensing, active and passive*. Artech House, Norwood, MA
- Ulaby F, Dubois PC, van Zyl J (1996) Radar mapping of surface soil moisture. *J Hydrol* 184(1–2):57–84
- Walker JP, Willgoose GR, Kalma JD (2001) One-dimensional soil moisture profile retrieval by assimilation of near-surface observations: a comparison of retrieval algorithms. *Adv Water Resour* 24:631–650
- Zhang Y-K, Schilling KE (2006) Effects of land cover on water table, soil moisture, evapotranspiration, and groundwater recharge: a field observation and analysis. *J Hydrol* 319(1–4): 328–338